

# Topological excitonic corner states and nodal phase in bilayer quantum spin Hall insulators

Zheng-Rong Liu,<sup>1</sup> Lun-Hui Hu,<sup>2</sup> Chui-Zhen Chen,<sup>3</sup> Bin Zhou,<sup>1</sup> and Dong-Hui Xu<sup>1,\*</sup>

<sup>1</sup>Department of Physics, Hubei University, Wuhan 430062, China

<sup>2</sup>Department of Physics, the Pennsylvania State University, University Park, PA, 16802, USA

<sup>3</sup>Institute for Advanced Study and School of Physical Science and Technology, Soochow University, Suzhou 215006, China.  
(Dated: February 28, 2025)

Interaction induced topological states remain one of the fascinating phases in condensed matter physics. The exciton condensate has recently sparked renewed interest due to the discovery of new candidate materials and its driving force to realize exotic topological states. In this work, we explore the exciton orders induced high-order topology in the bilayer quantum spin Hall insulators, and find that the topological excitonic corner states can be realized by tuning the gate and magnetic field. When an in-plane Zeeman field is applied to the system, two or four excitonic boundary-obstructed corner states emerge in the bilayer system for distinct possible  $s$ -wave excitonic pairings. Besides, we also find a two-dimensional excitonic Weyl nodal phase, which supports flat band edge states connecting the bulk Weyl nodes.

**Introduction.**—Excitonic insulator [1–4], predicted in the 1960s, is an unconventional insulating state formed by the condensation of excitons (bound electron-hole pairs) stemming from the Coulomb interaction between electrons and holes in the conduction and valence bands, respectively. An excitonic insulator is analogous to a Bardeen-Cooper-Schrieffer superconductor that results from the condensation of electron Cooper pairs developed near the Fermi surface. Candidate materials for excitonic insulators previously studied include quantum well bilayers [5], quantum Hall bilayers [6, 7], Ta<sub>2</sub>NiSe<sub>5</sub> [8–13], and 1T-TiSe<sub>2</sub> [14–17]. After the discovery of topological insulators, excitonic insulators with topologically non-trivial properties have been investigated intensively [18–33]. Particularly, a few representative topological exciton condensates, including the time-reversal invariant  $s$ -wave topological exciton condensate and the time-reversal breaking topological exciton condensate with  $p$ -wave pairing, have been predicted in HgTe/CdTe [23] and InAs/GaSb [24] quantum wells, respectively. Importantly, the evidence for the existence of topological excitonic insulator state has been reported experimentally in InAs/GaSb quantum wells [34, 35].

Recently, the concept of topological insulators was generalized, and a novel topological phase of matter dubbed higher-order topological insulator [36–41] was established. Compared to the well-known topological insulators, higher-order topological insulators exhibit an unusual form of bulk-boundary correspondence. For instance, a second-order topological insulator in two dimensions exhibits topological gapless boundary states at its zero-dimensional boundary corners, in contrast to a conventional two-dimensional (2D) first-order topological insulator which features topologically protected gapless states at its one-dimensional edge. So far, higher-order topology has been explored in various physical systems [42–90], and particularly Majorana zero-energy corner modes [63–65] were found in superconducting systems. Yet, the topological exciton condensates known to date belong to the first-order topological phases, and the study of higher-order topology in exciton condensates is still missing. Given the similarity of

excitonic insulators to superconductors, it is highly desirable to explore higher-order topology in exciton condensates in a realistic system.

In this work, we demonstrate that topological corner states, which are considered as a smoking-gun signature for 2D second-order topological insulators, can be realized in the bilayer quantum spin Hall insulators with  $s$ -wave interlayer excitonic pairings. The bilayer quantum spin Hall insulators can be constructed by two coupled HgTe/CdTe quantum wells, where the Dirac mass can be tuned by varying the thickness of the central HgTe layers in the quantum wells. For the bilayer system with the negative Dirac mass, four topological excitonic corner states are generated by applying an in-plane Zeeman field. By making use of the  $\mathbf{k} \cdot \mathbf{p}$  edge theory, we found that excitonic corner states originate from the edge mass domain walls formed by the interplay of the excitonic order and the Zeeman field. For the case of the positive Dirac mass, however only two topological excitonic corner states emerge. In addition, we show that an intriguing 2D excitonic nodal phase, which supports flat band edge states connecting the bulk Weyl nodes, could also be realized in this system. Our study suggests that exciton condensates can serve as a new platform to host higher-order topological insulating and topological nodal phases.

**Excitonic corner states for the negative Dirac mass.**— We report that a high-order topological excitonic insulator can be achieved in the bilayer quantum spin Hall insulators by tuning the bias voltage and in-plane Zeeman field. The low-energy effective Hamiltonian of the gated bilayer quantum spin Hall insulators in the momentum space is given by

$$H_{\text{QSH}}(\mathbf{k}) = M(\mathbf{k})\sigma_z + A(k_x\sigma_x s_z + k_y\sigma_y) - \frac{V}{2}\tau_z, \quad (1)$$

where the basis is  $c_{\mathbf{k}l}^\dagger = (c_{\mathbf{k}l\alpha\uparrow}^\dagger, c_{\mathbf{k}l\alpha\downarrow}^\dagger, c_{\mathbf{k}l\beta\uparrow}^\dagger, c_{\mathbf{k}l\beta\downarrow}^\dagger)$ ,  $\alpha$  and  $\beta$  are different orbital degrees of freedom with opposite parity,  $\uparrow$  and  $\downarrow$  represent electron spin, and  $l = 1, 2$  is the layer index.  $s_{x,y,z}$ ,  $\sigma_{x,y,z}$  and  $\tau_{x,y,z}$  are the Pauli matrices acting on the spin, orbital and layer degrees of freedom, respectively.  $\tau_0$ ,  $\sigma_0$  and  $s_0$  are the  $2 \times 2$  identity matrices.  $M(\mathbf{k}) = M - B(k_x^2 + k_y^2)$ , where the Dirac mass parameter  $M$  determines the topological insulator phase. And  $V$  is

\* donghuixu@hubu.edu.cn

the bias potential. When  $V = 0$ , this Hamiltonian is exactly two copies of the Bernevig-Hughes-Zhang (BHZ) model [91] that describes the HgTe/CdTe quantum wells. The topologically nontrivial phase of the BHZ model on a square lattice exists when  $0 < M/(2B/a^2) < 2$  with the lattice constant  $a$ . We assume the spatial separation between these two layers to be sufficiently large so that the single-particle tunneling between layers can be neglected. In subsequent calculations, the following parameters remain unchanged,  $A = 275 \text{ meV} \cdot \text{nm}$ ,  $B = -1300 \text{ meV} \cdot \text{nm}^2$ , and the lattice constant is  $a = 20 \text{ nm}$ . For our purpose, we set  $M = -3 \text{ meV}$  in this section. In this case, each layer contributes a Kramers pair of helical gapless edge states as shown in Fig. 1(a).

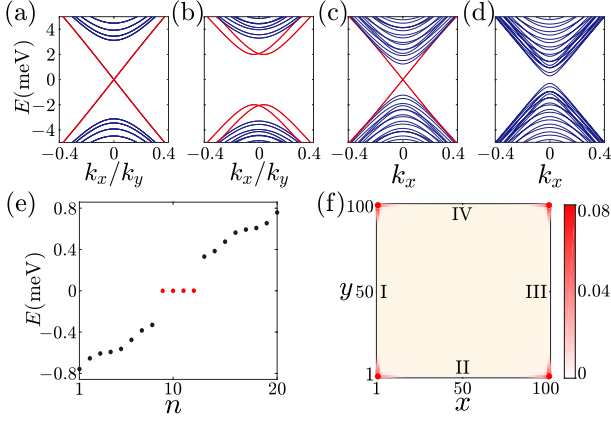


FIG. 1. Band structure of a ribbon geometry for (a)  $V = \Delta_X = h_x = 0$ , (b)  $V = 1 \text{ meV}$ ,  $\Delta_X = 2 \text{ meV}$ ,  $h_x = 0$ , (c)  $V = 1 \text{ meV}$ ,  $\Delta_X = 2 \text{ meV}$ ,  $h_x = 2.06 \text{ meV}$ , and (d)  $V = 1 \text{ meV}$ ,  $\Delta_X = 2 \text{ meV}$ ,  $h_x = 3 \text{ meV}$ . In (a) and (b), open boundary conditions along the  $x$ -direction or  $y$ -direction give rise to the same results. We take the open boundary condition in the  $y$ -direction. (e) Energy spectrum of an  $L_x \times L_y = 100 \times 100$  square-shaped sample exhibiting four ingap corner states marked by the red dots. (f) Probability distribution of corner states.

By turning on the electric bias  $V$ , an electron Fermi surface and a hole Fermi surface are created on layer 1 and layer 2, respectively. A coherent exciton condensation can be induced by the interlayer Coulomb interaction at the mean-field level. Throughout this paper, we focus on the time-reversal invariant  $s$ -wave exciton pairings which should be the leading order from the mean-field decomposition of the screened interlayer Coulomb interaction. In general, the  $s$ -wave excitonic order parameters could provide an energy gain to the system, which can be expressed as  $H_I = \Delta_X \tau_i \sigma_j s_k$  with  $\Delta_X$  the excitonic gaps and the subscripts  $i, j, k = 0, x, y, z$ . We have assumed the excitonic order parameters are momentum independent due to the short-range interaction. There are four relevant interlayer excitonic order parameters preserving the time-reversal symmetry, which are proportional to  $\tau_x \sigma_z s_0$ ,  $\tau_y \sigma_z s_z$ ,  $\tau_y \sigma_x s_x$ , and  $\tau_y \sigma_x s_y$ . Among these order parameters, it was found that the  $\tau_x \sigma_z s_0$ -type and  $\tau_y \sigma_z s_z$ -type orders can open a topological energy gap in the semimetallic bilayer HgTe/CdTe quantum wells i.e.,  $M = 0$ , resulting in a helical topological excitonic insulator characterized by the  $\mathbb{Z}_2$  topological invariant, while the  $\tau_y \sigma_x s_x$ -type and  $\tau_y \sigma_x s_y$ -type pairings only lead to a topo-

logically trivial energy gap in the case of  $M = 0$  [23].

Next we consider the case of  $M < 0$  with the  $\tau_y \sigma_x s_x$ -type interlayer excitonic order. The  $\tau_y \sigma_x s_y$ -type order will give rise to the similar results, which is not discussed here. In the bilayer system, these two pairs of helical edge states are not stable and gapped out by the excitonic order depicted in Fig. 1(b). When an in-plane Zeeman field  $h_x$  is applied along the  $x$ -direction, we can see that the quasiparticle edge gap along the  $k_x$ -direction closes as shown in Fig. 1(c) and reopens as  $h_x$  increases [see Fig. 1(d)]. Whereas, during this process, we verified that the edge gap along the  $k_y$ -direction doesn't close but only has a slight change in its amplitude. When two different types of edge gaps are formed along the  $x$  and  $y$  directions, we calculate the energy spectrum for a finite-sized square sample as shown in Fig. 1(e). Due to the sign change of the topological masses on two neighboring edges, four zero-energy boundary-obstructed midgap states appear, and they are located at the four corners of the square sample by observing the probability density [as shown in Fig. 1(f)].

Next, we discuss the above observed midgap states are exactly the topological excitonic corner states. To unveil their topological property, we calculate the edge polarization by using the Wilson loop operators [37, 40, 49]. For a ribbon geometry with  $N_y$  unit cells in the  $y$ -direction and  $N_{\text{orb}}$  degrees of freedom per unit cell, we express Wilson loop operator  $W_{x, k_x}$  on a path along the  $k_x$ -direction as  $W_{x, k_x} = F_{x, k_x + (N_x - 1)\Delta k_x} \cdots F_{x, k_x + \Delta k_x} F_{x, k_x}$ , where  $[F_{x, k_x}]^{mn} = \langle u_{k_x + \Delta k_x}^m | u_{k_x}^n \rangle$  with the step  $\Delta k_x = 2\pi/N_x$ , and  $|u_{k_x}^n\rangle$  denotes the occupied Bloch functions with  $n = 1, \dots, N_{\text{occ}}$ .  $N_{\text{occ}} = N_{\text{orb}} N_y / 2$  is the number of occupied bands. And  $W_{x, k_x}$  satisfies the following eigenvalue equation

$$W_{x, k_x} | \nu_{x, k_x}^j \rangle = e^{i2\pi\nu_x^j} | \nu_{x, k_x}^j \rangle, \quad (2)$$

where  $j = 1, \dots, N_{\text{occ}}$ . We can define the Wannier Hamiltonian  $H_{W_x}(k_x)$  as  $W_{x, k_x} \equiv e^{iH_{W_x}(k_x)}$ , of which the eigenvalues  $2\pi\nu_x$  correspond to the Wannier spectrum. The tangential polarization as a function of  $R_y$  is given as [37, 40, 49]

$$p_x(R_y) = \sum_{j=1}^{N_{\text{occ}} \times N_y} \rho^j(R_y) \nu_x^j, \quad (3)$$

where  $\rho^j(R_y) = \frac{1}{N_x} \sum_{k_x, \alpha, n} |[u_{k_x}^n]^{R_y, \alpha} [\nu_{k_x}^j]^n|^2$  is the probability density.  $[u_{k_x}^n]^{R_y, \alpha}$  with  $\alpha = 1, \dots, N_{\text{orb}}$ ,  $R_y = 1, \dots, N_y$  represents the components of the occupied states, and  $[\nu_{x, k_x}^j]^n$  is the  $n$ -th component of  $|\nu_{x, k_x}^j\rangle$ . The edge polarization at the  $y$ -normal edge is defined by  $p_x^{\text{edge}, y} = \sum_{R_y=1}^{N_y/2} p_x(R_y)$ . To fix the sign of the polarization, we add a perturbation term  $\delta\tau_y \sigma_x s_y$  in our calculations. Similarly, we can derive  $\nu_y$  and  $p_y^{\text{edge}, x}$ . We plot the Wannier spectra  $\nu_x$  and  $\nu_y$  as a function of  $h_x$  in Figs. 2(a) and 2(b), respectively. When the in-plane Zeeman field is larger than the critical  $h_x^c$ , the topological excitonic corner states appear. Correspondingly, the Wannier spectrum  $\nu_x$  has a pair of values pinned at  $1/2$ , resulting in half quantized edge polarization  $p_x^{\text{edge}, y}$  shown in Fig. 2(c). In contrast,  $p_y^{\text{edge}, x}$  remains vanishing even for  $h_x > h_x^c$ . It indicates that

the excitonic corner states originate from the quantized edge polarization  $p_x^{\text{edge},y}$ .

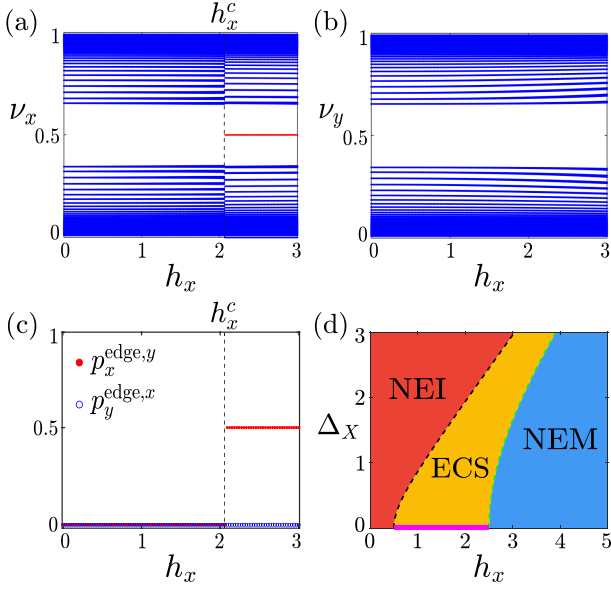


FIG. 2. (a), (b) Wannier spectra  $\nu_y$  and  $\nu_x$  versus  $h_x$ . (c) Edge polarization  $p_x^{\text{edge},y}$  and  $p_y^{\text{edge},x}$  along  $y$ -normal and  $x$ -normal edges, respectively. In (a)-(c),  $V = 1$  meV and  $\Delta_X = 2$  meV are used. (d) Phase diagram for topological excitonic corner states in the  $yx$ -type exciton condensation. The red color region marked by NEI stands for the normal excitonic insulator, the orange region marked by ECS denotes the region that supports topological excitonic corner states, and the blue region means a normal excitonic metal. For  $\Delta_X = 0$  and  $h_x > |V|/2$ , the edge states are gapped along the  $x$ -direction but remain gapless along the  $y$ -direction, which is marked by the solid magenta line  $\Delta_X$  is the  $s$ -wave exciton pairing gap and  $h_x$  is the strength of the Zeeman field along the  $x$ -direction. The dashed lines are phase boundaries determined by the topological condition for excitonic corner states  $\frac{1}{2}\sqrt{|V|^2 + 4\Delta_X^2} < h_x < \frac{1}{2}\sqrt{(2M + |V|)^2 + 4\Delta_X^2}$ , which agree well with the numerical results.

**Edge theory.**— To provide an intuitive picture to the appearance of excitonic corner states, we construct the edge theory [63] to analyze the topological mass on each edge. For simplicity, we focus on the  $V = 0$  case. The low-energy Hamiltonian of the exciton condensate around the  $\Gamma$  point

$$H(\mathbf{k}) = A(k_x\sigma_x s_z + k_y\sigma_y) + [M - B(k_x^2 + k_y^2)]\sigma_z + \Delta_X\tau_y\sigma_x s_x + h_x s_x. \quad (4)$$

We firstly consider a semi-infinite geometry occupying the space  $x \geq 0$  for edge I. In the spirit of  $\mathbf{k} \cdot \mathbf{p}$  theory, we replace  $k_x \rightarrow -i\partial_x$  and divide the Hamiltonian into  $H = H_0(-i\partial_x) + H_p(k_y)$ , in which

$$\begin{aligned} H_0(-i\partial_x) &= -iA\sigma_x s_z \partial_x + (M + B\partial_x^2)\sigma_z, \\ H_p(k_y) &= Ak_y\sigma_y + \Delta_X\tau_y\sigma_x s_x, \end{aligned} \quad (5)$$

where all the  $k_y^2$ -terms have been omitted, and  $h_x = 0$  for edge I. So we can solve  $H_0$  first, and regard  $H_p$  as a perturbation, which is justified when the exciton gap is small comparing to the energy gap. The eigenvalue equation  $H_0\psi_\alpha(x) =$

$E_\alpha\psi_\alpha(x)$  can be solved under the the boundary condition  $\psi_\alpha(0) = \psi_\alpha(+\infty) = 0$ . A straightforward calculation gives four degenerate solutions with  $E_\alpha = 0$ , whose eigenstates can be written in the following form

$$\psi_\alpha(x) = N_x \sin(\kappa_1 x) e^{-\kappa_2 x} e^{ik_y y} \chi_\alpha, \quad (6)$$

where the normalization constant  $N_x = 2\sqrt{\kappa_2(\kappa_1^2 + \kappa_2^2)}/\kappa_1^2$  with  $\kappa_1 = \sqrt{(4BM - A^2)/4B^2}$  and  $\kappa_2 = -A/2B$ . The eigenvectors  $\chi_\alpha$  are determined by  $\sigma_y s_z \chi_\alpha = -\chi_\alpha$ . Here we choose

$$\begin{aligned} \chi_1 &= |\sigma_y = -1\rangle \otimes |\uparrow\rangle \otimes |\tau_z = +1\rangle, \\ \chi_2 &= |\sigma_y = +1\rangle \otimes |\downarrow\rangle \otimes |\tau_z = +1\rangle, \\ \chi_3 &= |\sigma_y = -1\rangle \otimes |\uparrow\rangle \otimes |\tau_z = -1\rangle, \\ \chi_4 &= |\sigma_y = +1\rangle \otimes |\downarrow\rangle \otimes |\tau_z = -1\rangle. \end{aligned} \quad (7)$$

In this basis set, the matrix elements of the perturbation  $H_p(k_y)$  are represented as

$$H_{I,\alpha\beta}(k_y) = \int_0^{+\infty} dx \psi_\alpha^\dagger(x) H_p(k_y) \psi_\beta(x), \quad (8)$$

the effective low-energy Hamiltonian in a more compact form for the edge I is

$$H_I = -Ak_y s_z - \Delta_X \tau_y s_y, \quad (9)$$

Similarly, for edges II, III and IV, we obtain

$$\begin{aligned} H_{II} &= -Ak_x s_z - \Delta_X \tau_y s_x + h_x s_x, \\ H_{III} &= Ak_y s_z - \Delta_X \tau_y s_y, \\ H_{IV} &= Ak_x s_z - \Delta_X \tau_y s_x + h_x s_x. \end{aligned} \quad (10)$$

To be more clear, we introduce a unitary transformation  $U = \frac{1}{\sqrt{2}} \begin{pmatrix} i & -i \\ 1 & 1 \end{pmatrix}$ , then the edge Hamiltonians read

$$\begin{aligned} \tilde{H}_I &= -Ak_y s_z + \Delta_X \tau_z s_y, \\ \tilde{H}_{II} &= -Ak_x s_z + \Delta_X \tau_z s_x + h_x s_x, \\ \tilde{H}_{III} &= Ak_y s_z + \Delta_X \tau_z s_y, \\ \tilde{H}_{IV} &= Ak_x s_z + \Delta_X \tau_z s_x + h_x s_x. \end{aligned} \quad (11)$$

Now the edge Hamiltonians are block-diagonal. The effective masses of edges I and III are  $M_I = M_{III} = \Delta_X$ , while the effective masses of edges II and IV in the two blocks are  $M_{II} = M_{IV} = \Delta_X + h_x, h_x - \Delta_X$ . Therefore,  $(\Delta_X - h_x)\Delta_X < 0$  is the topological criteria to realize the topological excitonic corner states when  $V = 0$ . Consequently, the effective edge masses of the two adjacent boundaries have different sign, so mass domain walls appear at the intersection of these boundaries, which results in zero-energy excitonic modes.

In Fig. 2(d), we present the phase diagram of the bilayer system with the  $\tau_y\sigma_x s_x$ -type exciton condensate which is subjected to the in-plane Zeeman field  $h_x$ . The topological excitonic corner state phase (ECS) occupies the regime between the normal excitonic insulator phase (NEI) and the normal

excitonic metal phase (NEM). Here, the phase boundaries can be determined by the gap closing of the bulk at  $h_x = \frac{1}{2}\sqrt{|V|^2 + 4\Delta_X^2}$  and  $h_x = \frac{1}{2}\sqrt{(2M + |V|)^2 + 4\Delta_X^2}$ , which agree well with the numerical results. The topological region becomes narrower by increasing the voltage  $V$ . Therefore, the topological excitonic corner states, characterized by the quantized edge polarization, can be realized by tuning the gate and in-plane Zeeman field.

**Excitonic corner states and nodal phase for the positive Dirac mass.**— Next, we discuss if we can still realize the topological excitonic corner states on the bilayer system without band inversion occurring in each layer, where all the edge states are trivially fully gapped. For the  $\tau_x\sigma_zs_0$ -type exciton condensate, the in-plane Zeeman field can also generate excitonic corner states even when  $H_{\text{QSH}}$  has non-negative mass  $M \geq 0$ . For our purpose, we set  $M = 3$  meV in this section. Note that the bilayer system is a semiconductor in the absence of excitonic orders. The numerical calculation shows the in-plane Zeeman field  $h_x$  induces two excitonic corner states located at the left and right corners for a diamond-shaped sample [see Fig. 3(a)]. Although the Zeeman field breaks time-reversal symmetry,  $h_x$  preserves the 2-fold rotation symmetry about the  $x$ -axis  $C_{2x} = i\sigma_zs_x$ .

The first Brillouin zone (BZ) has a rotation-invariant line  $k_y = 0$  preserving the  $C_{2x}$  symmetry. We can adopt the mirror winding number [92] along this line to characterize the topological properties of this type of excitonic corner states. In this line,  $H(k_x, k_y = 0)$  is invariant under the operation of  $C_{2x}$ . The discrete version of  $H(k_x, 0)$  has the following form

$$H(k_x, 0) = \frac{A}{a} \sin(k_x a) \sigma_x s_z + M(k_x, 0) \sigma_z + h_x s_x - \frac{V}{2} \tau_z + \Delta_X \tau_x \sigma_z, \quad (12)$$

where  $M(k_x, 0) = M - \frac{B}{a^2} [2 - 2 \cos(k_x a)]$ .  $C_{2x}$  has two fourfold degenerate eigenvalues of  $\pm 1$ , the eigenvectors of  $\pm 1$  are  $1/\sqrt{2} |a\rangle \otimes (|\downarrow\rangle \pm |\uparrow\rangle) \otimes |T\rangle, 1/\sqrt{2} |b\rangle \otimes (|\downarrow\rangle \mp |\uparrow\rangle) \otimes |T\rangle, 1/\sqrt{2} |a\rangle \otimes (|\downarrow\rangle \pm |\uparrow\rangle) \otimes |B\rangle, 1/\sqrt{2} |b\rangle \otimes (|\downarrow\rangle \mp |\uparrow\rangle) \otimes |B\rangle$ , where  $|a\rangle$  ( $|b\rangle$ ),  $|\uparrow\rangle$  ( $|\downarrow\rangle$ ) and  $|T\rangle$  ( $|B\rangle$ ) are the basis vectors acting on the orbit, spin and layer subspaces, respectively. Due to the conversing of  $C_{2x}$ , we project  $H(k_x, 0)$  into the mirror-even (odd) subspaces corresponding to  $\pm 1$ , i.e.,  $H(k_x, 0) = H_+(k_x, 0) \oplus H_-(k_x, 0)$  And the block Hamiltonians read

$$H_{\pm}(k_x, 0) = [M(k_x, 0) \pm h_x] \sigma_z - \frac{V}{2} \tau_z - \frac{A}{a} \sin(k_x a) \sigma_x + \Delta_X \tau_x \sigma_z. \quad (13)$$

In the first BZ, along the mirror-invariant line  $k_y = 0$ , we consider the Wilson loop operator  $W_{\pm, k_x}$ . The mirror winding number  $\nu_{\pm}$  can be evaluated by [92]

$$\nu_{\pm} = \frac{1}{i\pi} \log(\det[W_{\pm, k_x}]) \bmod 2. \quad (14)$$

When the excitonic corner states emerge, the mirror winding number  $\nu_+ = \nu_- = 1$ .

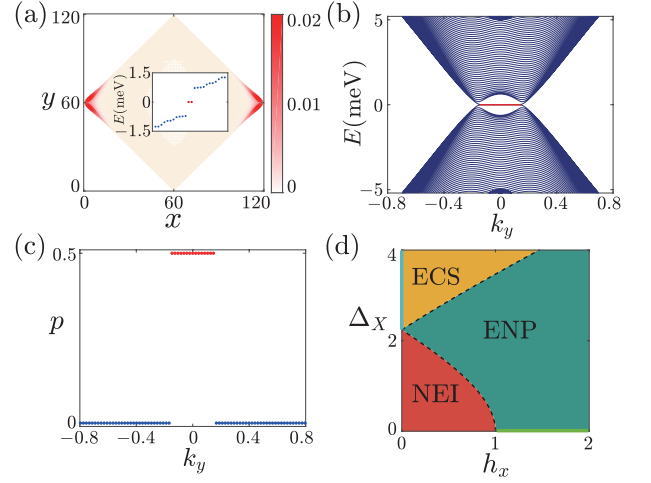


FIG. 3. (a) Probability distribution of excitonic corner states. Inset: energy spectrum. (b) Energy dispersion of the nodal phase for a ribbon geometry with open boundary condition along the  $x$ -direction. (c) Bulk polarization of nodal phase as a function of  $k_y$ . (d) Phase diagram of  $\tau_x\sigma_zs_0$ -type exciton condensation under the in-plane Zeeman field. The red regime marked by ENP represents the excitonic nodal phase. Same as the Fig. 2(d), the red color region marked by NEI stands for the normal exciton insulator, the orange region marked by ECS denotes the excitonic corner state phase. The solid green line means the normal metal driven by  $h_x$ , while the solid cyan line denotes helical excitonic insulator induced by the  $\tau_x\sigma_zs_0$ -type pairing. In (a), (b) and (c), we set  $V = 4$  meV,  $\Delta_X = 5$  meV,  $h_x = 3$  meV for (b) and (c), and  $h_x = 1$  meV for (a). In all plots,  $M = 3$  meV.

Now let us discuss the excitonic order induced nodal phase in the bilayer system. In the case of the  $\tau_x\sigma_zs_0$ -type exciton pairing, a nodal phase with Weyl nodes along the  $k_y$ -axis emerges. The excitonic nodal phase hosts flat band edge states as shown in Fig. 3(b). By treating  $k_y$  as a parameter, the Hamiltonian is effectively reduced to  $H_{k_y}(k_x)$ . In order to characterize the topological properties of nodal phase, we use the Wilson loop method to calculate the bulk polarization of the system. For fixed  $k_y$ , we consider the Wilson loop operator in the  $x$ -direction  $W_{x, k_x}$ , then the Wannier center  $\nu_x^j$  is obtained by the following equation

$$W_{x, k_x} \left| \nu_{x, k_x}^j \right\rangle = e^{i2\pi\nu_x^j} \left| \nu_{x, k_x}^j \right\rangle. \quad (15)$$

Then, for fixed  $k_y$ , the bulk polarization can be defined as  $p = \sum_j \nu_x^j \bmod 1$ . In Fig. 3(c), we plot the calculated bulk polarization as a function of  $k_y$ . We can see that the polarization is quantized to  $1/2$  between two nodes. Therefore, the topology of the nodal phase can be characterized by the  $k_y$ -dependent polarization.

Furthermore, the phase diagram for  $xz0$ -type exciton condensate on the plane of  $\Delta_X$  and  $h_x$  is shown in Fig. 3(d). By numerically observing the gap closing of the bulk, we define the phase boundaries. The boundary between the exciton corner states (ECS) and the exciton nodal phase (ENP) is explicitly determined by  $h_x = -M + \sqrt{\Delta_X^2 + |V|^2}/4$ , while the boundary between the normal exciton insulator (NEI)

and the exciton nodal phase is determined by  $h_x = M - \sqrt{\Delta_x^2 + |V|^2} / 4$ .

**Conclusion and discussion.**—In this work, we have identified two types of excitonic corner states in the gated bilayer quantum spin Hall insulator model with  $s$ -wave exciton pairings in the presence of the in-plane Zeeman field. We also found an excitonic nodal phase with the flat-band edge states in this system. Considering these exotic topological phases, our work will stimulate more investigations on higher-order topology and topological nodal phases in exciton condensates.

Different from superconducting pairings, excitonic pairings don't need to possess particle-hole symmetry. Therefore, excitonic corner states can appear at the finite energy, which is in contrast to Majorana corner states. In this paper, the excitonic corner states are pinned to zero energy as we use a particle-hole symmetric bilayer quantum spin Hall insulator model. When removing particle-hole symmetry, we can still have midgap excitonic corner states, but they will be shifted to

the finite energy.

Additionally, we mainly focus on the corner states created in the time-reversal invariant singlet  $s$ -wave exciton condensates hereinbefore. In this case, an in-plane Zeeman field is necessary to create the excitonic corner states. Whereas, we would like to point out that Kramers pairs of corner states could be generated in this bilayer system without applying a Zeeman field when time-reversal invariant  $d$ -wave exciton pairings are formed.

**Acknowledgments.**—D.-H.X. was supported by the NSFC (under Grant Nos. 12074108 and 11704106). B.Z. was supported by the NSFC (under Grant No. 12074107) and the program of outstanding young and middle-aged scientific and technological innovation team of colleges and universities in Hubei Province (under Grant No. T2020001). C.-Z.C. was funded by the NSFC (under Grant No. 11974256) and the NSF of Jiangsu Province (under Grant No. BK20190813). D.-H.X. also acknowledges the financial support of the Chutian Scholars Program in Hubei Province.

- 
- [1] N. F. Mott, “The transition to the metallic state,” *Philosophical Magazine* **6**, 287–309 (1961).
- [2] R. S. Knox, “Theory of excitons,” *Solid State Phys. Suppl.* **5**, 100 (1963).
- [3] L. V. K. Keldysh and Y. V. Kopayev, “Possible instability of the semimetallic state toward Coulomb interaction,” *Fiz. Tverd. Tela* **6**, 2791 (1964).
- [4] D. Jérôme, T. M. Rice, and W. Kohn, “Excitonic insulator,” *Phys. Rev.* **158**, 462–475 (1967).
- [5] M. M. Fogler, L. V. Butov, and K. S. Novoselov, “High-temperature superfluidity with indirect excitons in van der Waals heterostructures,” *Nat. Comm.* **5**, 1–5 (2014).
- [6] J. I. A. Li, T. Taniguchi, K. Watanabe, J. Hone, and C. R. Dean, “Excitonic superfluid phase in double bilayer graphene,” *Nat. Phys.* **13**, 751–755 (2017).
- [7] Xiaomeng Liu, Kenji Watanabe, Takashi Taniguchi, Bertrand I. Halperin, and Philip Kim, “Quantum Hall drag of exciton condensate in graphene,” *Nat. Phys.* **13**, 746–750 (2017).
- [8] Y. F. Lu, H. Kono, T. I. Larkin, A. W. Rost, T. Takayama, A. V. Boris, B. Keimer, and H. Takagi, “Zero-gap semiconductor to excitonic insulator transition in  $\text{Ta}_2\text{NiSe}_5$ ,” *Nat. Comm.* **8**, 1–7 (2017).
- [9] Daniel Werdehausen, Tomohiro Takayama, Marc Höppner, Gelon Albrecht, Andreas W. Rost, Yangfan Lu, Dirk Manske, Hidenori Takagi, and Stefan Kaiser, “Coherent order parameter oscillations in the ground state of the excitonic insulator  $\text{Ta}_2\text{NiSe}_5$ ,” *Sci. Adv.* **4**, eaap8652 (2018).
- [10] Y. Wakisaka, T. Sudayama, K. Takubo, T. Mizokawa, M. Arita, H. Namatame, M. Taniguchi, N. Katayama, M. Nohara, and H. Takagi, “Excitonic insulator state in  $\text{Ta}_2\text{NiSe}_5$  probed by photoemission spectroscopy,” *Phys. Rev. Lett.* **103**, 026402 (2009).
- [11] T. Kaneko, T. Toriyama, T. Konishi, and Y. Ohta, “Orthorhombic-to-monoclinic phase transition of  $\text{Ta}_2\text{NiSe}_5$  induced by the Bose-Einstein condensation of excitons,” *Phys. Rev. B* **87**, 035121 (2013).
- [12] Koudai Sugimoto, Satoshi Nishimoto, Tatsuya Kaneko, and Yukinori Ohta, “Strong coupling nature of the excitonic insulator state in  $\text{Ta}_2\text{NiSe}_5$ ,” *Phys. Rev. Lett.* **120**, 247602 (2018).
- [13] Giacomo Mazza, Malte Rösner, Lukas Windgätter, Simone Latini, Hannes Hübener, Andrew J. Millis, Angel Rubio, and Antoine Georges, “Nature of symmetry breaking at the excitonic insulator transition:  $\text{Ta}_2\text{NiSe}_5$ ,” *Phys. Rev. Lett.* **124**, 197601 (2020).
- [14] Anshul Kogar, Melinda S. Rak, Sean Vig, Ali A. Husain, Felix Flicker, Young Il Joe, Luc Venema, Greg J. MacDougall, Tai C. Chiang, Eduardo Fradkin, Jasper van Wezel, and Peter Abbamonte, “Signatures of exciton condensation in a transition metal dichalcogenide,” *Science* **358**, 1314–1317 (2017).
- [15] H. Cercellier, C. Monney, F. Clerc, C. Battaglia, L. Despont, M. G. Garnier, H. Beck, P. Aebi, L. Patthey, H. Berger, and L. Forró, “Evidence for an excitonic insulator phase in 1T- $\text{TiSe}_2$ ,” *Phys. Rev. Lett.* **99**, 146403 (2007).
- [16] Tatsuya Kaneko, Yukinori Ohta, and Seiji Yunoki, “Exciton-phonon cooperative mechanism of the triple- $q$  charge-density-wave and antiferroelectric electron polarization in  $\text{TiSe}_2$ ,” *Phys. Rev. B* **97**, 155131 (2018).
- [17] Chuan Chen, Bahadur Singh, Hsin Lin, and Vitor M. Pereira, “Reproduction of the charge density wave phase diagram in 1T- $\text{TiSe}_2$  exposes its excitonic character,” *Phys. Rev. Lett.* **121**, 226602 (2018).
- [18] B. Seradjeh, J. E. Moore, and M. Franz, “Exciton condensation and charge fractionalization in a topological insulator film,” *Phys. Rev. Lett.* **103**, 066402 (2009).
- [19] Ningning Hao, Ping Zhang, and Yupeng Wang, “Topological phases and fractional excitations of the exciton condensate in a special class of bilayer systems,” *Phys. Rev. B* **84**, 155447 (2011).
- [20] Gil Young Cho and Joel E. Moore, “Quantum phase transition and fractional excitations in a topological insulator thin film with Zeeman and excitonic masses,” *Phys. Rev. B* **84**, 165101 (2011).
- [21] Dagim Tilahun, Byounghak Lee, E. M. Hankiewicz, and A. H. MacDonald, “Quantum Hall superfluids in topological insulator thin films,” *Phys. Rev. Lett.* **107**, 246401 (2011).
- [22] D. K. Efimkin, Yu. E. Lozovik, and A. A. Sokolik, “Electron-hole pairing in a topological insulator thin film,” *Phys. Rev. B* **86**, 115436 (2012).
- [23] Jan Carl Budich, Björn Trauzettel, and Paolo Michetti, “Time

- reversal symmetric topological exciton condensate in bilayer HgTe quantum wells,” *Phys. Rev. Lett.* **112**, 146405 (2014).
- [24] D. I. Pikulin and T. Hyart, “Interplay of exciton condensation and the quantum spin Hall effect in InAs/GaSb bilayers,” *Phys. Rev. Lett.* **112**, 176403 (2014).
- [25] Ke Chen and Ryuichi Shindou, “Chiral topological excitons in a Chern band insulator,” *Phys. Rev. B* **96**, 161101 (2017).
- [26] Yichen Hu, Jörn W. F. Venderbos, and C. L. Kane, “Fractional excitonic insulator,” *Phys. Rev. Lett.* **121**, 126601 (2018).
- [27] Qizhong Zhu, Matisse Wei-Yuan Tu, Qingjun Tong, and Wang Yao, “Gate tuning from exciton superfluid to quantum anomalous Hall in van der Waals heterobilayer,” *Sci. Adv.* **5**, eaau6120 (2019).
- [28] Lun-Hui Hu, Rui-Xing Zhang, Fu-Chun Zhang, and Congjun Wu, “Interacting topological mirror excitonic insulator in one dimension,” *Phys. Rev. B* **102**, 235115 (2020).
- [29] Rui Wang, Onur Erten, Baigeng Wang, and D.Y. Xing, “Prediction of a topological  $p + ip$  excitonic insulator with parity anomaly,” *Nat. Commun.* **10**, 1–9 (2019).
- [30] Daniele Varsano, Maurizia Palummo, Elisa Molinari, and Massimo Rontani, “A monolayer transition-metal dichalcogenide as a topological excitonic insulator,” *Nat. Nanotechnol.* **15**, 367–372 (2020).
- [31] Andrea Blason and Michele Fabrizio, “Exciton topology and condensation in a model quantum spin Hall insulator,” *Phys. Rev. B* **102**, 035146 (2020).
- [32] E. Perfetto and G. Stefanucci, “Floquet topological phase of nondriven  $p$ -wave nonequilibrium excitonic insulators,” *Phys. Rev. Lett.* **125**, 106401 (2020).
- [33] Zhiyuan Sun and Andrew J. Millis, “Topological charge pumping in excitonic insulators,” [arXiv:2008.00134 \[cond-mat.mes-hall\]](https://arxiv.org/abs/2008.00134).
- [34] Lingjie Du, Xinwei Li, Wenkai Lou, Gerard Sullivan, Kai Chang, Junichiro Kono, and Rui-Rui Du, “Evidence for a topological excitonic insulator in InAs/GaSb bilayers,” *Nat. Comm.* **8**, 1–8 (2017).
- [35] W. Yu, V. Clericò, C. Hernández Fuentevilla, Xiaoyan Shi, Y. Jiang, D. Saha, W. K. Lou, K. Chang, D. H. Huang, G. Gumbs, *et al.*, “Anomalously large resistance at the charge neutrality point in a zero-gap InAs/GaSb bilayer,” *New J. Phys.* **20**, 053062 (2018).
- [36] Fan Zhang, C. L. Kane, and E. J. Mele, “Surface state magnetization and chiral edge states on topological insulators,” *Phys. Rev. Lett.* **110**, 046404 (2013).
- [37] Wladimir A. Benalcazar, B. Andrei Bernevig, and Taylor L. Hughes, “Quantized electric multipole insulators,” *Science* **357**, 61–66 (2017).
- [38] Josias Langbehn, Yang Peng, Luka Trifunovic, Felix von Oppen, and Piet W. Brouwer, “Reflection-symmetric second-order topological insulators and superconductors,” *Phys. Rev. Lett.* **119**, 246401 (2017).
- [39] Zhida Song, Zhong Fang, and Chen Fang, “ $(d-2)$ -dimensional edge states of rotation symmetry protected topological states,” *Phys. Rev. Lett.* **119**, 246402 (2017).
- [40] Wladimir A. Benalcazar, B. Andrei Bernevig, and Taylor L. Hughes, “Electric multipole moments, topological multipole moment pumping, and chiral hinge states in crystalline insulators,” *Phys. Rev. B* **96**, 245115 (2017).
- [41] Frank Schindler, Ashley M. Cook, Maia G. Vergniory, Zhi-jun Wang, Stuart S. P. Parkin, B. Andrei Bernevig, and Titus Neupert, “Higher-order topological insulators,” *Sci. Adv.* **4**, eaat0346 (2018).
- [42] Motohiko Ezawa, “Higher-order topological insulators and semimetals on the breathing Kagome and pyrochlore lattices,” *Phys. Rev. Lett.* **120**, 026801 (2018).
- [43] Motohiko Ezawa, “Topological switch between second-order topological insulators and topological crystalline insulators,” *Phys. Rev. Lett.* **121**, 116801 (2018).
- [44] Max Geier, Luka Trifunovic, Max Hoskam, and Piet W. Brouwer, “Second-order topological insulators and superconductors with an order-two crystalline symmetry,” *Phys. Rev. B* **97**, 205135 (2018).
- [45] Eslam Khalaf, “Higher-order topological insulators and superconductors protected by inversion symmetry,” *Phys. Rev. B* **97**, 205136 (2018).
- [46] Motohiko Ezawa, “Strong and weak second-order topological insulators with hexagonal symmetry and  $\mathbb{Z}_3$  index,” *Phys. Rev. B* **97**, 241402(R) (2018).
- [47] Flore K. Kunst, Guido van Miert, and Emil J. Bergholtz, “Lattice models with exactly solvable topological hinge and corner states,” *Phys. Rev. B* **97**, 241405(R) (2018).
- [48] Guido van Miert and Carmine Ortix, “Higher-order topological insulators protected by inversion and rotoinversion symmetries,” *Phys. Rev. B* **98**, 081110(R) (2018).
- [49] S. Franca, J. van den Brink, and I. C. Fulga, “An anomalous higher-order topological insulator,” *Phys. Rev. B* **98**, 201114(R) (2018).
- [50] Yizhi You, Trithip Devakul, F. J. Burnell, and Titus Neupert, “Higher-order symmetry-protected topological states for interacting bosons and fermions,” *Phys. Rev. B* **98**, 235102 (2018).
- [51] Sander H. Kooi, Guido van Miert, and Carmine Ortix, “Inversion-symmetry protected chiral hinge states in stacks of doped quantum Hall layers,” *Phys. Rev. B* **98**, 245102 (2018).
- [52] Luka Trifunovic and Piet W. Brouwer, “Higher-order bulk-boundary correspondence for topological crystalline phases,” *Phys. Rev. X* **9**, 011012 (2019).
- [53] Feng Liu, Hai-Yao Deng, and Katsunori Wakabayashi, “Helical topological edge states in a quadrupole phase,” *Phys. Rev. Lett.* **122**, 086804 (2019).
- [54] Haiyan Fan, Baizhan Xia, Liang Tong, Shengjie Zheng, and Dejie Yu, “Elastic higher-order topological insulator with topologically protected corner states,” *Phys. Rev. Lett.* **122**, 204301 (2019).
- [55] Zhijun Wang, Benjamin J. Wieder, Jian Li, Binghai Yan, and B. Andrei Bernevig, “Higher-order topology, monopole nodal lines, and the origin of large Fermi arcs in transition metal dichalcogenides  $XTe_2$  ( $X=Mo,W$ ),” *Phys. Rev. Lett.* **123**, 186401 (2019).
- [56] Xian-Lei Sheng, Cong Chen, Huiying Liu, Ziyu Chen, Zhi-Ming Yu, Y. X. Zhao, and Shengyuan A. Yang, “Two-dimensional second-order topological insulator in graphdiyne,” *Phys. Rev. Lett.* **123**, 256402 (2019).
- [57] Rui Chen, Chui-Zhen Chen, Jin-Hua Gao, Bin Zhou, and Dong-Hui Xu, “Higher-order topological insulators in quasicrystals,” *Phys. Rev. Lett.* **124**, 036803 (2020).
- [58] Dániel Varjas, Alexander Lau, Kim Pöyhönen, Anton R. Akhmerov, Dmitry I. Pikulin, and Ion Cosma Fulga, “Topological phases without crystalline counterparts,” *Phys. Rev. Lett.* **123**, 196401 (2019).
- [59] Chun-Bo Hua, Rui Chen, Bin Zhou, and Dong-Hui Xu, “Higher-order topological insulator in a dodecagonal quasicrystal,” *Phys. Rev. B* **102**, 241102 (2020).
- [60] Dumitru Călugăru, Vladimir Juričić, and Bitan Roy, “Higher-order topological phases: A general principle of construction,” *Phys. Rev. B* **99**, 041301 (2019).
- [61] Wladimir A. Benalcazar, Tianhe Li, and Taylor L. Hughes, “Quantization of fractional corner charge in  $C_n$ -symmetric higher-order topological crystalline insulators,” *Phys. Rev. B* **99**,

- 245151 (2019).
- [62] Martin Rodriguez-Vega, Abhishek Kumar, and Babak Seradjeh, “Higher-order Floquet topological phases with corner and bulk bound states,” *Phys. Rev. B* **100**, 085138 (2019).
- [63] Zhongbo Yan, Fei Song, and Zhong Wang, “Majorana corner modes in a high-temperature platform,” *Phys. Rev. Lett.* **121**, 096803 (2018).
- [64] Qiyue Wang, Cheng-Cheng Liu, Yuan-Ming Lu, and Fan Zhang, “High-temperature majorana corner states,” *Phys. Rev. Lett.* **121**, 186801 (2018).
- [65] Xiaoyu Zhu, “Tunable majorana corner states in a two-dimensional second-order topological superconductor induced by magnetic fields,” *Phys. Rev. B* **97**, 205134 (2018).
- [66] Vatsal Dwivedi, Ciarán Hickey, Tim Eschmann, and Simon Trebst, “Majorana corner modes in a second-order Kitaev spin liquid,” *Phys. Rev. B* **98**, 054432 (2018).
- [67] Yuxuan Wang, Mao Lin, and Taylor L. Hughes, “Weak-pairing higher order topological superconductors,” *Phys. Rev. B* **98**, 165144 (2018).
- [68] Tao Liu, James Jun He, and Franco Nori, “Majorana corner states in a two-dimensional magnetic topological insulator on a high-temperature superconductor,” *Phys. Rev. B* **98**, 245413 (2018).
- [69] Yanick Volpez, Daniel Loss, and Jelena Klinovaja, “Second-order topological superconductivity in  $\pi$ -junction Rashba layers,” *Phys. Rev. Lett.* **122**, 126402 (2019).
- [70] Xiao-Hong Pan, Kai-Jie Yang, Li Chen, Gang Xu, Chao-Xing Liu, and Xin Liu, “Lattice-symmetry-assisted second-order topological superconductors and Majorana patterns,” *Phys. Rev. Lett.* **123**, 156801 (2019).
- [71] Zhongbo Yan, “Higher-order topological odd-parity superconductors,” *Phys. Rev. Lett.* **123**, 177001 (2019).
- [72] Zhongbo Yan, “Majorana corner and hinge modes in second-order topological insulator/superconductor heterostructures,” *Phys. Rev. B* **100**, 205406 (2019).
- [73] S. Franca, D. V. Efremov, and I. C. Fulga, “Phase-tunable second-order topological superconductor,” *Phys. Rev. B* **100**, 075415 (2019).
- [74] Marc Serra-Garcia, Valerio Peri, Roman Süssstrunk, Osama R. Bilal, Tom Larsen, Luis Guillermo Villanueva, and Sebastian D. Huber, “Observation of a phononic quadrupole topological insulator,” *Nature (London)* **555**, 342–345 (2018).
- [75] Christopher W. Peterson, Wladimir A. Benalcazar, Taylor L. Hughes, and Gaurav Bahl, “A quantized microwave quadrupole insulator with topologically protected corner states,” *Nature* **555**, 346–350 (2018).
- [76] Haoran Xue, Yahui Yang, Fei Gao, Yidong Chong, and Baile Zhang, “Acoustic higher-order topological insulator on a kagome lattice,” *Nat. Mater.* **18**, 108–112 (2018).
- [77] Xiang Ni, Matthew Weiner, Andrea Alù, and Alexander B. Khanikaev, “Observation of higher-order topological acoustic states protected by generalized chiral symmetry,” *Nat. Mater.* **18**, 113–120 (2018).
- [78] Frank Schindler, Zhijun Wang, Maia G. Vergniory, Ashley M. Cook, Anil Murani, Shamashis Sengupta, Alik Yu Kasumov, Richard Deblock, Sangjun Jeon, Ilya Drozdov, *et al.*, “Higher-order topology in bismuth,” *Nat. Phys.* **14**, 918–924 (2018).
- [79] Stefan Imhof, Christian Berger, Florian Bayer, Johannes Brehm, Laurens W. Molenkamp, Tobias Kiessling, Frank Schindler, Ching Hua Lee, Martin Greiter, Titus Neupert, and Ronny Thomale, “Topoelectrical-circuit realization of topological corner modes,” *Nat. Phys.* **14**, 925–929 (2018).
- [80] Jiho Noh, Wladimir A. Benalcazar, Sheng Huang, Matthew J. Collins, Kevin P. Chen, Taylor L. Hughes, and Mikael C. Rechtsman, “Topological protection of photonic mid-gap defect modes,” *Nat. Photonics* **12**, 408–415 (2018).
- [81] Xiujuan Zhang, Hai-Xiao Wang, Zhi-Kang Lin, Yuan Tian, Biye Xie, Ming-Hui Lu, Yan-Feng Chen, and Jian-Hua Jiang, “Second-order topology and multidimensional topological transitions in sonic crystals,” *Nat. Phys.* **15**, 582–588 (2019).
- [82] S. N. Kempkes, M. R. Slot, J. J. van den Broeke, P. Capiod, W. A. Benalcazar, D. Vanmaekelbergh, D. Bercioux, I. Swart, and C. Morais Smith, “Robust zero-energy modes in an electronic higher-order topological insulator,” *Nat. Mater.* **18**, 1292–1297 (2019).
- [83] Sunil Mittal, Venkata Vikram Orre, Guanyu Zhu, Maxim A. Gorlach, Alexander Poddubny, and Mohammad Hafezi, “Photonic quadrupole topological phases,” *Nat. Photonics* **13**, 692–696 (2019).
- [84] Ashraf El Hassan, Flore K. Kunst, Alexander Moritz, Guillermo Andler, Emil J. Bergholtz, and Mohamed Bourennane, “Corner states of light in photonic waveguides,” *Nat. Photonics* **13**, 697–700 (2019).
- [85] Eunwoo Lee, Rokyoon Kim, Junyeong Ahn, and Bohm-Jung Yang, “Two-dimensional higher-order topology in monolayer graphdiyne,” *npj Quantum Materials* **5**, 1 (2020).
- [86] Koji Kudo, Tsuneya Yoshida, and Yasuhiro Hatsugai, “Higher-order topological Mott insulators,” *Phys. Rev. Lett.* **123**, 196402 (2019).
- [87] Yuanfeng Xu, Zhida Song, Zhijun Wang, Hongming Weng, and Xi Dai, “Higher-order topology of the axion insulator  $\text{EuIn}_2\text{As}_2$ ,” *Phys. Rev. Lett.* **122**, 256402 (2019).
- [88] Changming Yue, Yuanfeng Xu, Zhida Song, Hongming Weng, Yuan-Ming Lu, Chen Fang, and Xi Dai, “Symmetry-enforced chiral hinge states and surface quantum anomalous Hall effect in the magnetic axion insulator  $\text{Bi}_{2-x}\text{Sm}_x\text{Se}_3$ ,” *Nat. Phys.* **15**, 577–581 (2019).
- [89] Yafei Ren, Zhenhua Qiao, and Qian Niu, “Engineering corner states from two-dimensional topological insulators,” *Phys. Rev. Lett.* **124**, 166804 (2020).
- [90] Ya-Jie Wu, Junpeng Hou, Yun-Mei Li, Xi-Wang Luo, Xiaoyan Shi, and Chuanwei Zhang, “In-plane Zeeman-field-induced Majorana corner and hinge modes in an  $s$ -wave superconductor heterostructure,” *Phys. Rev. Lett.* **124**, 227001 (2020).
- [91] B. Andrei Bernevig, Taylor L. Hughes, and Shou-Cheng Zhang, “Quantum spin Hall effect and topological phase transition in  $\text{HgTe}$  quantum wells,” *Science* **314**, 1757–1761 (2006).
- [92] Moon Jip Park, Youngkuk Kim, Gil Young Cho, and Sung-Bin Lee, “Higher-order topological insulator in twisted bilayer graphene,” *Phys. Rev. Lett.* **123**, 216803 (2019).